University of South-Eastern Norway
Faculty of Technology, Natural Sciences and Maritime Sciences
–
Master's Thesis
Study programme: Master of Science in Micro and Nano Systems Technology
Spring/Autumn 2023

Diani Indrachapa Muhandiram

Doping and etching processes of iCL – CNT for high energy density supercapacitors

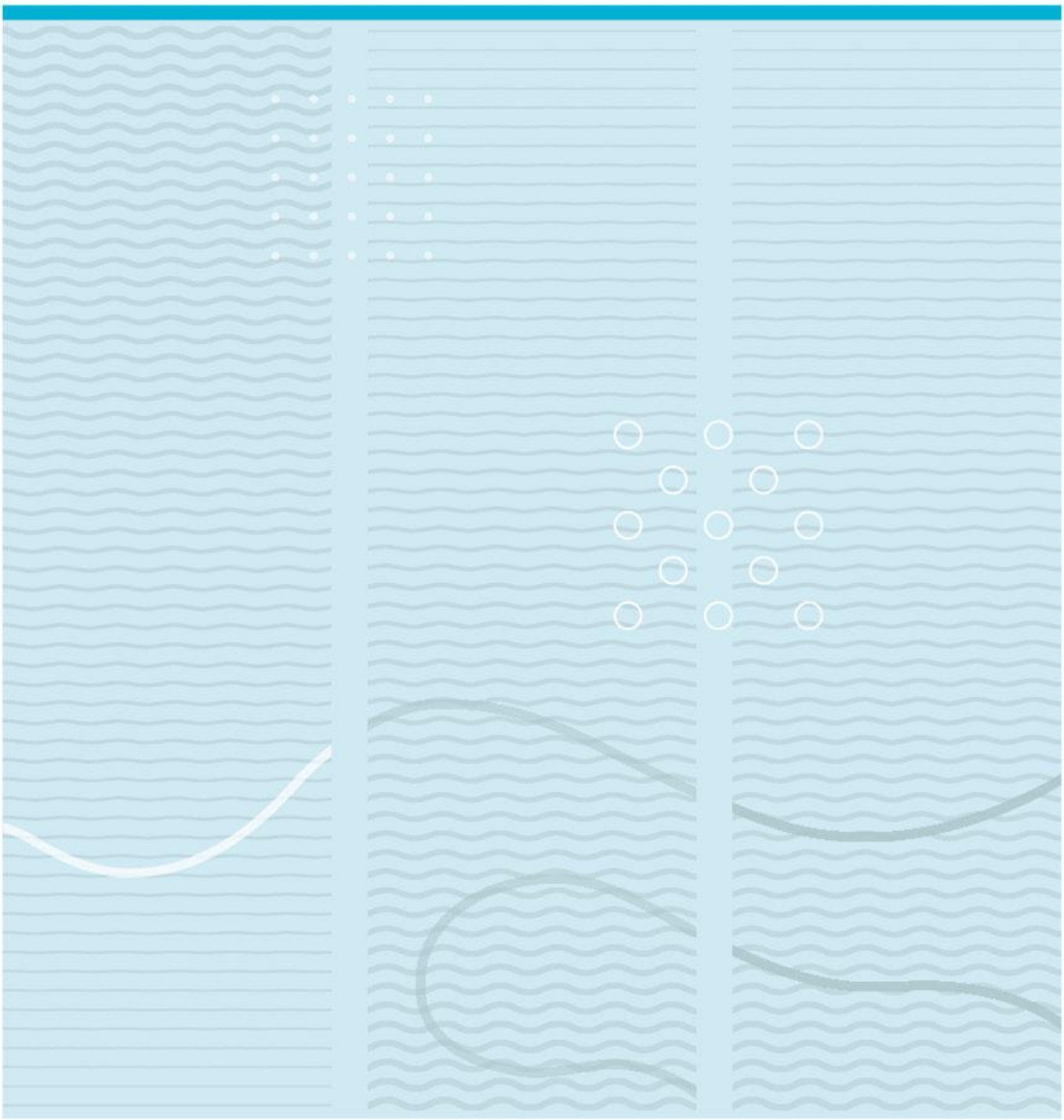

University of South-Eastern Norway
Faculty of Technology, Natural Sciences and Maritime Sciences
Department of Microsystems.
Raveien 215
NO-3184 Borre, Norway

http://www.usn.no

Summary

The purpose of this study is to investigate the defects resulting from the etching and N_2 doping process which have the potential to increase the surface area of carbon nanotubes (CNTs), and consequently enhance the energy density for energy storage devices. The synthesis of CNTs was carried out on an aluminium (Al) substrate followed by activation through KOH etching and controlled air oxidation at high temperatures to promote porosity. Although KOH etching yielded promising results in terms of porosity, however, the temperature used exceeded the melting point of the Al substrate. As a result, the CNT films needed to be scraped off from the substrate. The effect of oxidation of CNTs on capacitance and morphology was investigated. The results revealed an ideal oxidation time of less than 25 minutes which can increase the specific capacitance. However, longer durations may damage the CNTs and consequently reduce the capacitance. Moreover, the study compared the morphology and capacitance characteristics of CNTs synthesized using Ar and N_2 as carrier gas and we found that N_2 is a more cost-effective, practical, and feasible option for industrial applications. Notably, a higher gravimetric capacitance with a value of 68F/g was obtained using N_2 as a carrier gas. However, further investigations are needed to determine the underlying cause of this improvement. In summary, this study highlights practical techniques for enhancing the surface area and porosity of CNTs, with and without a substrate, particularly for the development of high energy density supercapacitors.

Preface

This study was conducted in the Department of Systems of the University of South-Eastern Norway, under Dr. Xuyuan Chen. Throughout this journey, I have had the privilege of working with brilliant mentors, colleagues, and friends.

I would like to take this opportunity to express my sincere gratitude to my main supervisor Dr. Xuyuan Chen, and my co-supervisors and mentors Per Øhlckers, Dr. Raghu Ummethala, Dr. Pai Lu, and all the nanoCaps employees for the invaluable guidance, feedback, and encouragement they gave me throughout this research process. I would also like to express my utmost appreciation to the Research Council of Norway for funding the project NORFAB III (project number: 295864), USN lab engineers, and all the other employees who helped me throughout the research period to obtain the best results for my experiments. Moreover, I'd like to thank my friends and colleagues who helped me to make this research a success.

Finally, I'd like to dedicate this study to my family who have provided me with love, support, and encouragement throughout my academic journey.

<Borre/22.05.2023>

<Diani Indrachapa Muhandiram>

Table of Contents

1 Introduction

In the modern world, the demand for high-performance energy storage devices is rapidly increasing for different applications. Although the performance of batteries is good, their capabilities are still subjected to certain limitations therefore, the novel focus is shifted towards developing supercapacitors (SCs) which employ electrochemical energy-storing method that enable higher power density. For improving the energy density of SCs, few factors such as surface porosity, pore size distribution, the thickness of the electrodes, etc. are more focused in the present energy storage research and industry development [1]. Carbon nanotubes (CNT) used as the electrode material of a SC has a long cycle life, improved energy density, and higher power density [2]. One of the advantages of using CNT compared to activated carbon (AC) is the high effective surface area of CNTs, and good electron conductivity. Due to the entangled tubular structural morphology of the CNT as opposed to the collection of carbon particles in AC, the mesopores in CNTs are interconnected which permits a continuous charge distribution throughout the effective surface area, resulting in a better performance giving higher specific capacitance values [3].

1.1 The scope of thesis

A supercapacitor typically comprises of two electrodes with electrode material on a current collector with a separator material in between [4]. Over the years, researchers have conducted numerous experiments on the improvement of the surface area of the electrode materials aiming a higher capacitance, thus, improved energy density for SCs [5], [6]. In addition to using CNT as an electrode material, some experiments have been conducted to create porosity on the nanotube surface with chemical and physical reactions aiming to obtain more larger surface area, resulting a significant improvement in the SC specific capacitance. Two primary methods to increase the surface area of CNTs are etching and doping of CNTs. Doping is an in-situ method that can be implemented during the growth of CNTs using Chemical Vapour Deposition (CVD) process. The most common materials used for doping are nitrogen [7], [8], and boron [9], however, one limitation of this method is that the defects occurring on the CNTs mostly are in the range of micropore or mesopore [10], which may not be effective to improve the energy density

of the supercapacitors in the presence of larger electrolyte ions, thus, resulting a lower specific capacitance than the one as expected. For ex-situ etching, common chemicals used include alkaline hydroxides [11], [12], acids [1], [2], and gases [13], [14]. It is essential to note that the most of these etching reactions typically occur at high temperatures, and higher thermal energy is required to break the bonds of chemicals and then to react with Carbon (C) atoms in the CNT structure. Additionally, most of these methods are focused on CNT powder without a substrate.

For industrial production of supercapacitors, growing CNTs on an Aluminium (Al) substrate is more efficient [15]. Therefore, if the etching and doping can be performed on the CNTs on the Al substrate, it would be an ideal strategy. Hence in this thesis, the focus was on improving the surface area of the CNT on the Al substrate by employing etching and doping methods. The CNTs were grown by atmospheric pressure chemical vapour deposition (APCVD) method with Ni nanoparticles as the catalyst. Catalyst selection is a crucial factor for CNT deposition in larger scale production as the catalyst needs to be highly effective [16], possesses a nano dimension [17], is prepared with a method that is compatible with the substrate and suitable for industrial-scale production. Considering all above facts, we use the magneto sputtering method to deposit Ni particles on Al substrate in this study.

1.2 Research approach

The primary objective of this study focused on finding a suitable method of the etching process at a temperature lower than the Al melting temperature with a minimal reactivity with the Al substrate. The study revealed that using nitrogen (N_2) gas as a doping source with thermal APCVD at 600^{o}C was not enough to break the triple bond in N_2 gas. However, both Argon (Ar) and N_2 were found to have a similar effect on CNT properties including specific capacitance and therefore, N_2 is more economical and feasible for the use in industrial production, hence it is a more favourable option than Ar. Furthermore, this study shows that the ex-situ etching with potassium hydroxide (KOH) at 700^{o}C without Al substrate, resulted in a certain degree of porous morphology on the CNT surface nonetheless, due to KOH reaction with carbon needed a higher temperature than Al substrate can withstand, another etching method was investigated. Therefore, the study

investigated air etching, which is a process that can be implemented at temperatures below 600^{o}C and has a minimal chemical reactivity with Al substrates, thereby, improving the porosity of CNTs to increase the surface area of the SC and compare the resulting improvement in specific capacitance.

1.3 Thesis structure

In this study, Chapter 1 introduces the related background and explanation of the research motivation, approach, and outline in brief.

Chapter 2 is an explanation in detail about the theoretical and recent research related to the topic. It contains the recent studies about supercapacitors, factors affecting the SC capacitance, and what methods have been used so far to improve the capacitance by modifying the surface morphology of the electrode material.

The experimental procedure implemented to improve the capacitance by enhancing the surface area is explained in Chapter 3. This contains the sample preparation, synthesis of CNT using two different carrier gases, two types of ex-situ etching methods, and the method of characterization.

Chapter 4 is the analysis of the obtained results in this study. Scanning Electron Microscope (SEM) and Fourier transform infrared (FTIR) spectroscopy were used for morphology analysis, and an electrochemical workstation was used to obtain Cyclic Voltammetry (CV) curves so that the capacitance could be calculated.

2 Background Studies

Background study related to the main thesis topic prior to and during the research is extremely important to understand the method of implementing the experiments regarding the topic and to analyse the results. It is also important to know the theoretical background of materials and other components being used, and their mechanical and chemical behaviour before doing an experiment.

This chapter is focusing on the theoretical background of CNTs and the synthesizing process of CNTs, a brief explanation of supercapacitors and their properties, and a theoretical and recent study of etching methods with pros and cons related to this study.

2.1 Carbon nanotubes

Carbon nanotubes are sp^2 hybridized bonded carbon atoms organized in a honeycomb structure, as a graphene sheet cylindrical tube. These sheets may assemble as a single layer of sheet tube or as multiple layers of sheets arranged together concentrically. Coaxial Multiwall Carbon Nanotubes (MWNT) were first observed through a Transmission Electron Microscope (TEM) in 1991 and Single Wall Nanotubes (SWNT) were first discovered in 1993. Typically, carbon nanotubes have a diameter of a few nanometers and the length could be in micrometers to millimeters range [18].

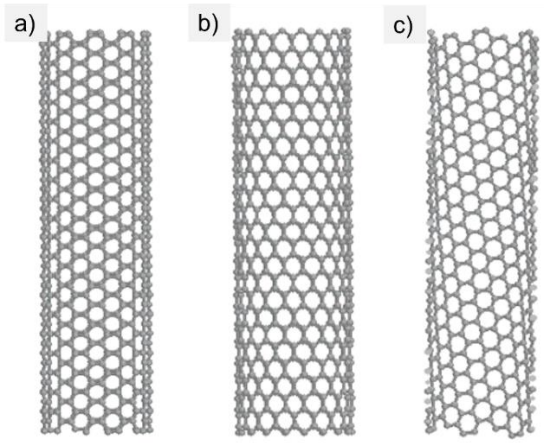

Figure 2-1: Schematic honeycomb structure of CNT with a) armchair b) zigzag c) chiral structures

Interconnected cross-linked carbon nanotubes (iCL-CNT) are created by forming covalent bonds between adjacent CNTs and creating a 3-dimensional network. It can be expected

for iCL-CNTs to have enhanced mechanical, chemical, and thermal properties in compared to pure CNTs [19].

2.2 CVD process and Catalyst

CNT can be synthesized in various methods and most of these methods require the use of a catalyst to break the carbon source and transform it in to sp^2 hybridized tube structure. The growth of the CNT will be initiated by catalyst nanoparticles, which function by splitting the carbon-carbon bond in a gaseous carbon source and forming a carbon-metal bond. The nanotube diameter is found to be highly influenced by the catalyst particle size [20].

The most common types of catalysts used are transition metallic catalysts such as iron (Fe), Cobalt (Co), and Nickel (Ni). Among these 3 catalysts, Lee et.al claims that Ni has the highest growth rate of CNTs, which is an important efficiency factor in the industrial production of CNTs for supercapacitors [16].

The most common and economical way of synthesis of CNTs is the thermal APCVD process. The main ingredients used in this process are a catalyst such as Ni, Fe or Co, etc., a gaseous carbon sources such as C_2H_2, CH_4, etc., H_2 as reduction gas, and a neutral carrier gas such as Ar or N_2. The process is done at a higher temperature, in a closed furnace by maintaining atmospheric pressure throughout the synthesis.

The CVD process for growing CNTs involves several steps. First, the precursor decomposes on the catalyst's surface, forming bonds with the catalyst. Then, carbon diffuses through the catalyst, which can result in the formation of either CNTs or amorphous carbon. Finally, gas-phase reactions of the precursor molecule can influence the growth process.

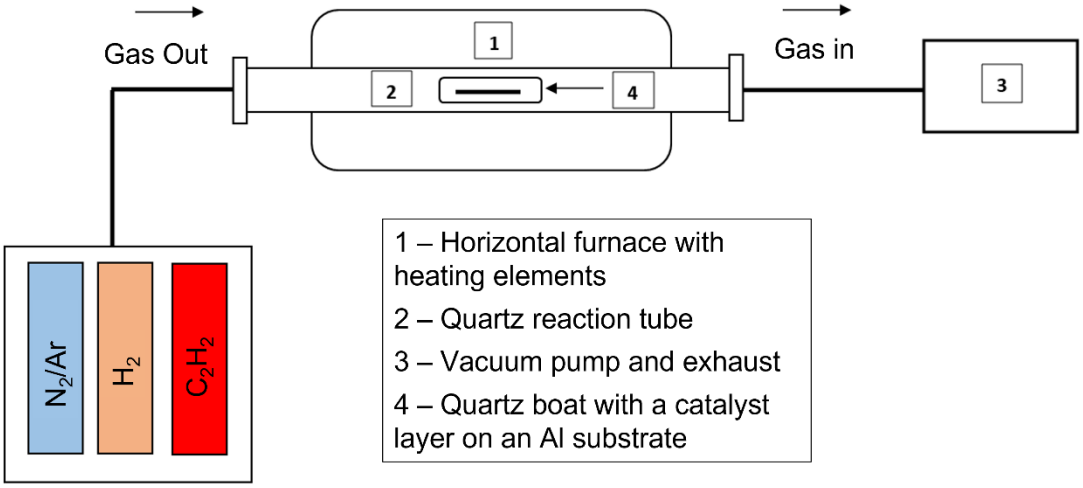

Figure 2-2: Schematic diagram of CVD reactor

The procedure involves introducing a neutral carrier gas into the system until it achieves the desired synthesis temperature eliminating all the oxygen from the system. The reason for this is that oxygen can cause oxidation during the synthesis of CNTs and the combustion with the gaseous carbon source like acetylene. The carrier gas is assisting the transportation of the gaseous carbon source and H_2 to the heating zone, and the gaseous carbon source will undergo thermal decomposition under elevated temperature with the aid of catalyst nanoparticles. The decomposition of the carbon source will generate into sp^2 hybridized tube structure, creating carbon nanotubes on the catalyst nanoparticles. The residual gases will be removed through the use of a vacuum pump throughout this process [21].

2.3 Supercapacitor background

A supercapacitor is a high-energy density storage device consisting of two electrodes with a current collector and electrode material, an electrolyte, and a separator in between. The performance of the SC depends on the factors such as surface area and other electrochemical properties of the electrode material, type and potential window of the electrolyte, ability of the filtration of the separator, etc. The supercapacitor is the most suitable option to store energy that goes through frequent charging and discharging cycles with a high current and short duration [22], [23].

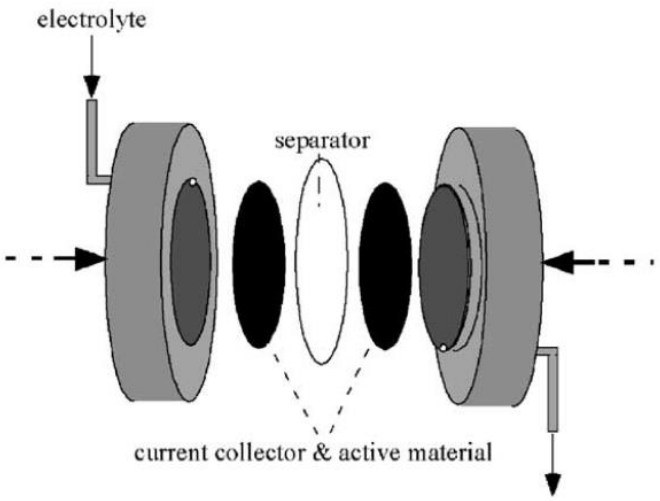

Figure 2-3: Schematic structure of a EDLC supercapacitor test cell [4].

The method of energy storing in a supercapacitor can be explained through the electrical double layer theory. There exist various proposed models regarding the storage of electric charge in a supercapacitor, with the most recent ones being the Stern model and the Muller method, which is an advancement of the Stern model. The basic Stern model consists of two distinct layers - the Helmholtz layer and the diffusion layer. Upon the application of an electric field to the capacitor, one of the current collector metals acquires a positive charge, thereby attracting the negative anions of the electrolyte, which results in the formation of a thin negative ion layer that balances out the positive charge on the metal. The opposite charge situation arises in the other electrode, leading to the formation of the Helmholtz layer. The second layer is composed of diffused ions that are not strictly attracted to the charged metal layer and can diffuse back into the electrolyte. These ions can alter their positions based on various factors such as the charge of the metal layer, the charge of the ions that remain in the electrolyte, and the effect of the other electrode. Together, these two layers constitute the electrical double layer (EDL) and are responsible for the charge storage mechanism in a supercapacitor [24].

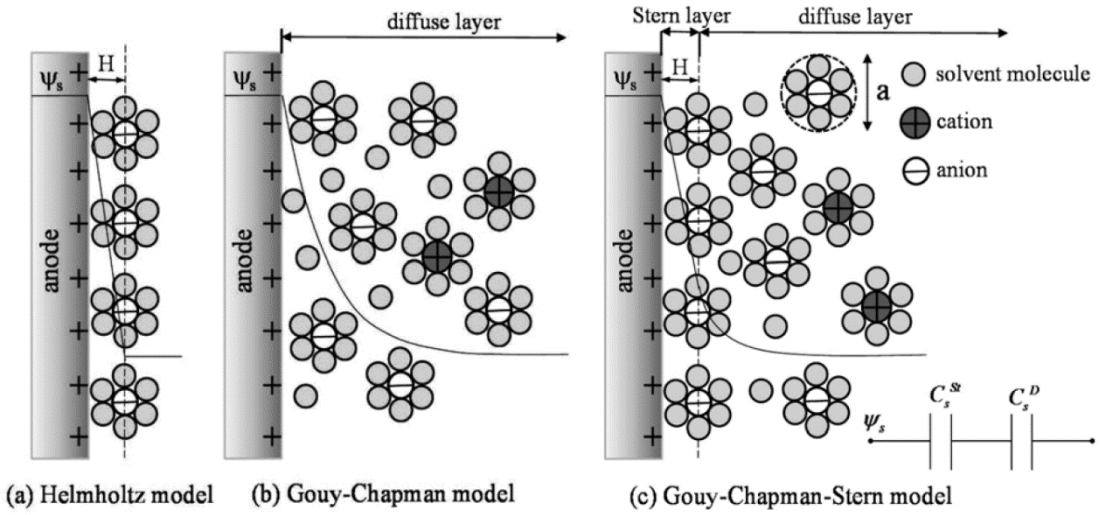

Figure 2-4: EDL models. (c) is considered to be the most accurate and H is the EDL distance proposed in model (a) [25].

Numerous techniques can be used to determine the specific capacitance of a supercapacitor. CV is one of the most widely used techniques. In this method, the SC is subjected to a changing potential within a predetermined potential that is set by the type of electrolyte, and the resulting change in charge and discharge current is plotted in accordance with that. The following formulas can be used to determine a SC's specific capacitance while taking into the account of the overall area under the CV curve [26].

Here i represents instantaneous current, dE/dt is scanning rate, (E2 – E1) is the upper limit potential.

$$C = \frac{dq}{dE} = \frac{dq}{dE} \times \frac{dt}{dE} = i \times \frac{dt}{dE} = \frac{i}{v} \quad \text{----- (1)}$$

$$C = \frac{i}{v} = \frac{{}^{1}/_{E2-E1}\int_{E1}^{E2} i(E)dE}{v \times 2} \quad \text{----- (2)}$$

Hence,

$$C_{Areal} = \frac{Total\ area\ under\ the\ curve(mA*V)}{2*scan\ rate(\frac{mV}{s})*Area\ of\ the\ electrode(cm2)*potential\ window(V)} \quad \text{----- (3)}$$

$$C_{Gravimetric} = \frac{Total\ area\ under\ the\ curve(mA*V)}{2*scan\ rate(\frac{mV}{s})*Active\ mass\ of\ the\ electrode\ (g)*potential\ window(V)} \quad \text{----- (4)}$$

The capacitance can be presented in a few different formats. Areal capacitance which is the specific capacitance per unit area (mF/cm^2) and gravimetric capacitance which is the specific capacitance per unit mass (F/g) are considered in this report.

2.4 CNT etching processes

2.4.1 Importance of etching CNTs for high energy density supercapacitors

Removing atoms or layers of materials and creating a form of defects on the surface of the material by using chemical or physical (ion bombardment) method is known as etching.

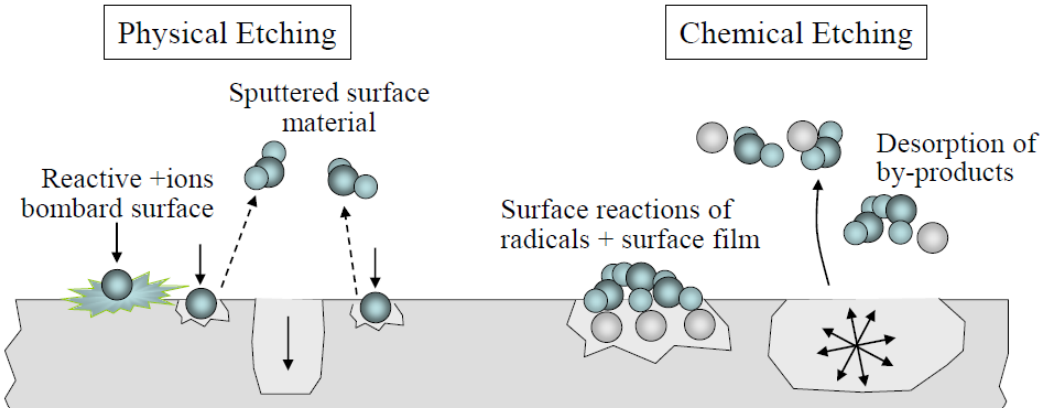

Figure 2-5: Chemical and Physical etching process of a material in an animated figure [27].

Etching increases the material porosity resulting in a higher surface area. CNT etching or most well-known as activation, gives a higher surface area to the electrode surface by creating scattered areas on the nanotube surface.

When the surface area is high (by higher porosity), the amount of charge that the surface can hold becomes high. Hence, the specific capacitance will be high. Therefore, it is important to have a high porosity in the electrode material of a supercapacitor.

2.4.2 Typical methods for etching the CNTs

The first focus was on etching the CNTs that were deposited on Aluminium (Al) and therefore, the etching should be done using a method that does not affect the Al substrate. However, after thorough research about the topic of etching of CNTs on an Al substrate, it was obvious that the temperature and chemicals used in the etching of CNTs

cannot be used with Al as Al has a low melting point of 660^{o}C and should not be exposed to higher temperatures than around 620^{o}C [28]. There was one etching method that could use directly on the CNTs grown on Al substrate which will be discussed in the upcoming chapters.

Mainly, CNT etching and doping can be discussed as follows.

2.4.2.1 In-situ Doping

In-situ doping is done while the CNT growth happens using a chemical vapour deposition (CVD) process. When it comes to doping, Nitrogen (N) and Boron (B) are the most frequently used atoms. Ayala *et al.* mentioned that the incorporation of a foreign atom to the CNT lattice will create structural defects which possibly create a higher porosity [7].

1. N doping into CNT

Czerw *et al.* mentioned that the N doped CNTs show a "bamboo type" structure with a slightly distorted surface on the CNTs with certain nano-level porous places due to N doping [10].

The size of the porous places might be an issue as, what they have observed is in the micropore range, which might not influence any difference in electrical properties if the pores are smaller than the electrolyte molecules used in supercapacitor applications. In conclusion, if doping can cause considerable defects in the structure of the nanotubes, it can also be considered as a method of increasing the specific capacitance of the supercapacitor. Apart from making defects by doping, Mofokeng *et al.* mentioned that the N doping will give pseudocapacitive properties to the electrode material making the EDL complete non-faradic process into a combination of faradic/diffusion and non-faradic methods [29].

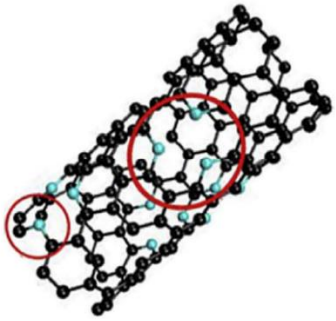

Figure 2-6: N doped CNT animated figure showing the micro/mesopores [7].

2. B doping into CNT

CNT can be doped with boron by introducing boron-containing material into the CVD process. Zhang *et al.* experimented on boron doped CNTs, which were prepared using Boric acid and CNTs mixed in different CNT: boric acid weight ratios and heating at 1000^{o}C for 4hrs and subjecting it to post-treatment. They have concluded that the B doping has a significant impact on the specific capacitance [9]. However, this method has limitations such as the usage of extremely high temperatures, therefore, this cannot be used on CNT grown on Al substrate. Additionally, some boron-containing chemicals are highly toxic.

2.4.2.2 Ex-situ Etching

When the etching of CNTs is performed after the CNT deposition process, as a post-treatment, it is referred to as ex-situ etching. This approach is the most common etching method of CNTs as it is relatively straightforward to implement unless CNTs are deposited on a metallic substrate. Most of the highly concentrated acids and highly concentrated bases can etch CNTs by reacting with carbon atoms.

1. Etching using alkaline hydroxides.

The most common alkaline hydroxide used for etching/activation of CNTs is potassium hydroxide (KOH) as it is non-toxic, environment friendly, and easy to handle. During KOH activation, alkali hydroxides are introduced to the system, and this is followed by hydrogen reduction and carbon oxidation, removing C atoms from the CNT structure, and leading to a porous structure. Therefore, by-product gases like H_2 need to be removed

carefully hence this process needs to be done in a high-temperature furnace with a vacuum system.

The main condition for this reaction to occur is a high temperature in the range of 700°C - 800°C and lower temperatures than these may not provide effective results. One of the main by-products is a CO_3^{2-} of the metal in the alkaline hydroxide, which needs to be removed from the CNTs after activation. Therefore, post-treatment is required to remove residual by-products using de-ionized (DI) water until the pH value of CNTs becomes neutral [11]. Residual by-products may affect the capacitance and morphology characterization.

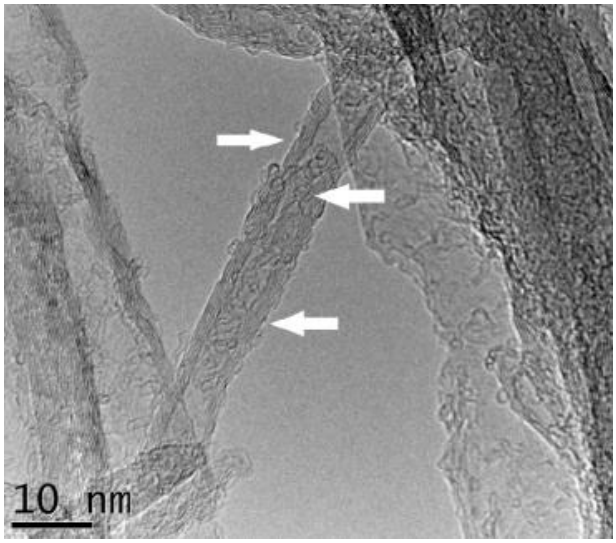

Figure 2-7: High resolution Transmission Electron Microscopy image of KOH activated CNT at 800°C for 2h. Micropores are shown from white arrows [12].

Zhang et al. experimented the impact of temperature on the creation of porous surfaces using KOH for a specified duration. The results showed that the temperatures under 500°C did not produce any significant change in the porosity compared to pristine CNT. However, temperatures above 600°C exhibit promising porosity, with the most favourable porous surface observed between 700°C – 800°C. It should be noted that the most favourable porous surface was obtained after a 2h activation period which may not be efficient for industrial-scale production. It can be observed that the pores that occurs in their experiment are in the micropore range [12].

2. Etching using acids.

Dai *et al.* have experimented the impact of HNO_3 at higher temperatures on CNTs. They have observed that higher HNO_3 concentrations, such as 5M and longer etching durations, such as 12h were necessary to achieve a higher degree of porosity on CNT structure [1]. Although the temperature used here is below the melting temperature of Al which enables its use on CNTs deposited on Al substrate, there are still a few drawbacks associated with this method. HNO_3 is a strong oxidizing agent which creates an oxide layer on Al and higher oxide layers influence the equivalent series resistance (ESR) of the supercapacitor. Additionally, the etching duration is extremely long which will be not efficient in industrial production.

Zięzio *et al.* have activated normal activated carbon using phosphoric acid and Hastak *et al.* have used it for CNT activation [2], [30]. The phosphoric acid activation with CNT is happening in two major steps. Removing water and other volatile materials and decomposing phosphoric which then reacts with carbon are those steps briefly.

Although again, since phosphoric is still an acid, it will react chemically with Al if the etching is done on CNTs deposited on Al.

3. Air Etching

Li et al. investigated the effect of air etching or thermal annealing in the air on CNTs. Pre-prepared CNT samples were put in a quartz tube furnace and were annealed in air at a temperature range of 480^{o}C – 750^{o}C for a duration of 20 minutes. They concluded that starting at 480°C and reaching a peak at 650°C, the surface area increased from this air etching. Higher temperatures caused a decrease in surface area. The use of CNTs directly, rather than in conjunction with a metallic substrate, for the subsequent manufacturing of the electrodes is a crucial consideration in this experimental approach [13].

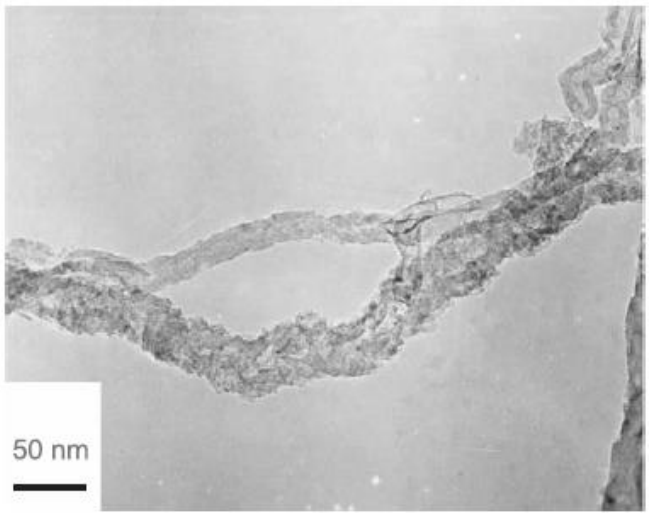

Figure 2-8: A TEM image of CNTs air etched at 540°C with porous surface [13].

Seo et al. conducted an experiment to investigate the effect of selective oxidation under 600°C on the porosity and electrochemical properties of CNTs. It was discovered that oxidation can make CNTs more porous and boost their specific capacitance. The higher porosity resulted in an increased number of active sites for the adsorption of electrolytic ions, thus enhancing the electrochemical performance of CNTs [31].

Wang et al. observed and suggested that compared with CO_2 and H_2O, O_2 has a low etching rate but, it is possible to make a porous surface on SWNT using air. Also, it is mentioned that the etching should be controlled with low time duration and 610°C [32].

At elevated temperatures, oxygen-containing air can react with carbon, resulting in the removal of carbon atoms from the surface of the material. This procedure causes the carbon material to develop a porous structure, increasing its surface area. However, it is crucial to state that the etching process must be performed under controlled conditions to prevent excessive removal of carbon atoms from the sample. Alternatively, complete reactions of all available carbon atoms in any structure in the material can be formed when exposed to reactant conditions such as extreme temperature and duration.

Apart from the etching of the carbon nanotube surface, because the reaction rate of C and O_2 depends on the C-C bond strength hence, air etching can be used to remove the amorphous carbon, defective carbon coatings, expose or remove residual catalyst

particles after catalytic CNT CVD synthesis. Prior to the etching of a CNT sample, any bond strength below C sp^2 hybrid structure may be removed [33].

One important fact about air etching relating to this study is that air etching can be done under the temperature of 660^oC which is the melting point of Al substrate and O_2 doesn't react with Al which will affect the supercapacitor properties. Therefore, air etching can be done to the CNT samples synthesized on the Al substrate without separating the CNT from the substrate.

Some CNT synthesizing methods can not only produce CNT but in addition, it can create unnecessary carbonaceous particles as well [34],[35]. This might be a disadvantage for gaining the maximum effect of the electrochemical properties of CNTs. Therefore, after the synthesis of CNTs, a purification method without affecting the CNTs is required.

C reaction with O_2 depends on the C atom bonding type and strength. Park et al. stated that the oxidation rate of CNT is much lower compared to the oxidation rate of the structures with pentagons, heptagons, and amorphous carbon. CNT has a hexagonal tubular structure [36]. Therefore, selective, carefully controlled oxidation can be used for purification without severely damaging the CNT structure.

3 Experimental Setup and Methodology

This chapter describes the complete explanation of experimental work steps implemented to investigate the research questions posed in this study. The methodology was designed to gather data that could be analyzed to answer research questions and test the hypotheses.

This chapter includes a systematic approach to sample preparation for CNT synthesis, growth of CNTs using Ar and N_2 as carrier gases through the APCVD process on Al substrate which was used directly as an electrode for a supercapacitor, ex-situ etching of grown CNTs without the Al substrate using KOH, ex-situ etching of CNTs synthesized on Al substrate using controlled air oxidation and material characterization stages to observe the morphology and capacitance differences.

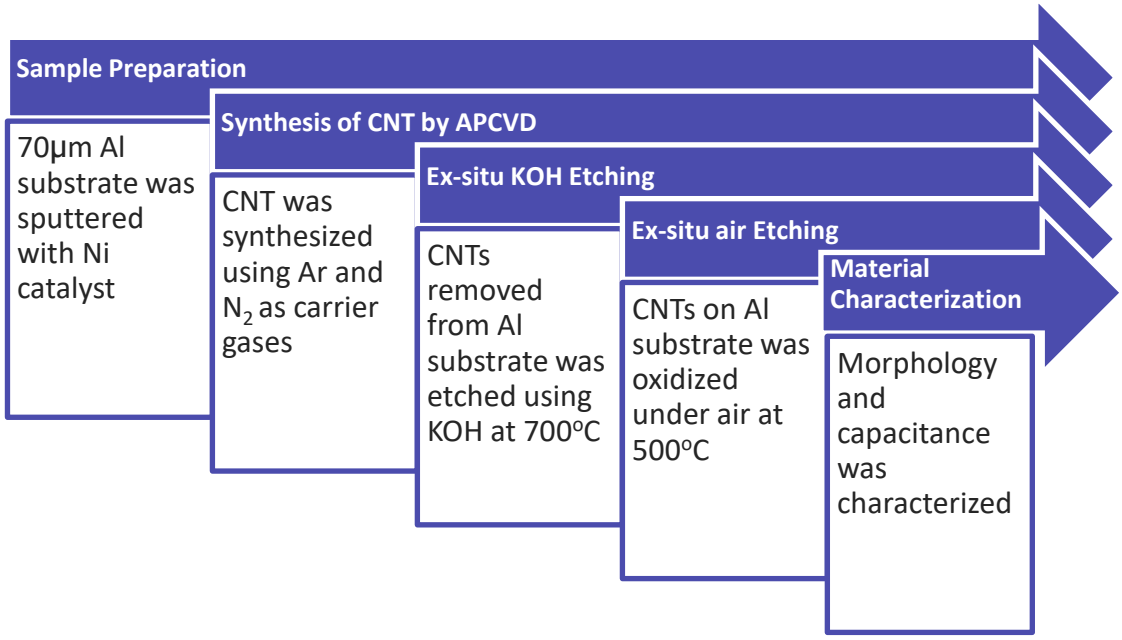

Figure 3-1: Schematic diagram of the workflow of this study

3.1 Growth of CNT on Al substrate with Ar and N_2 as carrier gas

In this study, industrially pre-etched 70µm Al foil from FOILTEC was used as a substrate. Al substrate with sputtered Ni was provided by a fellow master student. Prior to sputtering for catalyst deposition, the substrate was cleaned with acetone, followed by a

10-minute dip in iso-propanol, and finally, it was cleaned with De-ionized (DI) water. After drying with N_2, Ni was deposited using the magnetron sputtering machine (Sputter AJA - ATC 20x20x30) at room temperature. The thickness of the Ni layer specified in the machine was 100nm for a planar substrate, however, since the etched Al foil surface is not planar because of the surface porosity hence the actual Ni thickness may vary.

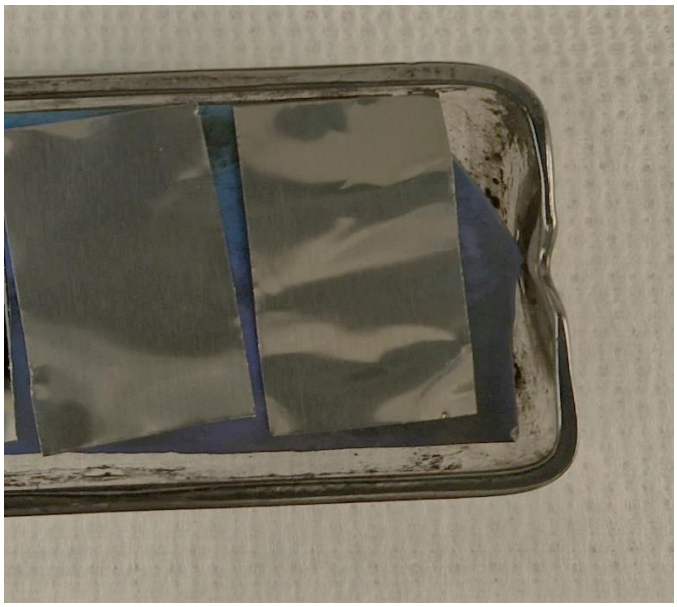

Figure 3-2: 70µm Al substrate with a sputtered Ni layer of 100nm machine specified planar surface thickness.

The previously prepared sample was used to grow CNT using thermal APCVD with both Ar and N_2 as a carrier gas for comparison. The sample was placed on a quartz boat. The APCVD process for synthesizing CNTs was done in a high-temperature horizontal vacuum tube furnace (GSL-1100X) at 600^{o}C for 1hrs using the gas composition of C_2H_2: H_2: Ar/N_2 = 20: 80: 100 SCCM. The carrier gas was sent through a water bubbler. The furnace was cooled under 200-300sccm N_2 flow for 1-2hrs before taking out the sample.

Hydrocarbon break at high temperature into C and H producing carbon free-radicals, and these radicals will attach to the Ni catalyst on the substrate creating the sp^2 hybridized C structure in a tubular form.

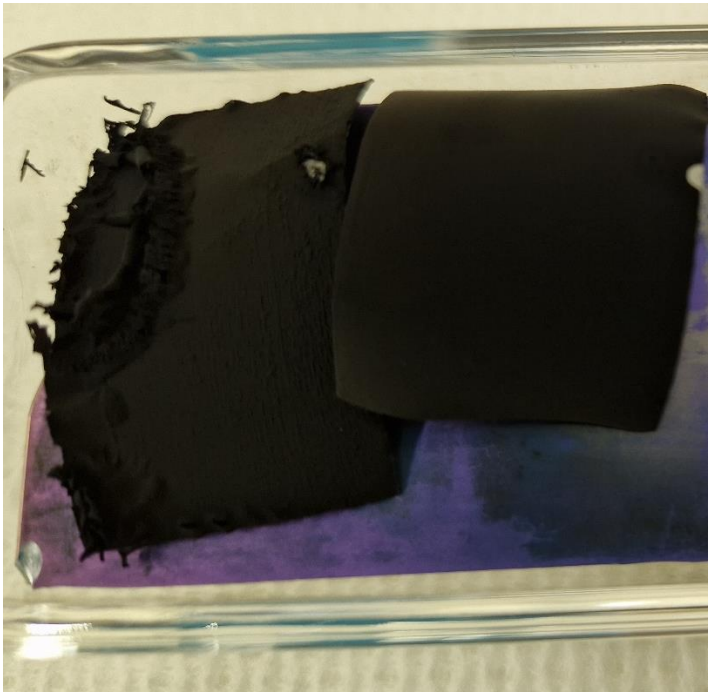

Figure 3-3: Synthesized CNT using N_2 as a carrier gas, on Al substrate with sputtered Ni as a catalyst.

3.2 CNT ex-situ KOH etching

The synthesized CNTs using APCVD on Al substrate was separated from the substrate. CNT powder was thoroughly mixed with potassium hydroxide powder (KOH) (Sigma-Aldrich) in 1:2 wt.% ratio and it was put in a quartz boat and was heated in high temperature vacuum tube furnace under 100sccm N_2 gas flow for a duration of 15 minutes under 700^{o}C temperature.

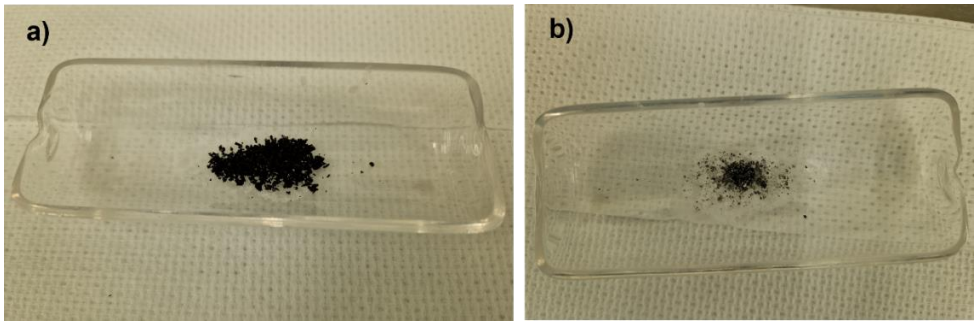

Figure 3-4: a) CNT: KOH 1:2 wt.% ratio mixer before etching b) The sample after KOH etching at 700^{o}C for 15 minutes.

The chemical reaction occurring during the etching of CNTs using KOH can be shown as follows.

$$6KOH + C \rightarrow 2K + 3H_2 + 2K_2CO_3 \text{ -------- } (3\text{-}1)$$

C from the sp^2 hybridized structure in CNTs are removed in the form of K_2CO_3 which is a water-soluble substance. These by-products were removed in the post treatment by washing the etched CNTs with DI water for few times [11].

3.3 CNT ex-situ air etching

Previously synthesized CNT samples using N_2 as the carrier gas were cut into 4 parts. The muffle furnace (High temperature furnace - LHT 02/17) was heated up to 500°C in normal air, and one sample was put in for 10min and the second one for 20min and the third for 25min.

At high temperatures, O_2 in air reacts with C atoms in CNT structure making the CNT surface porous. The chemical reaction for carbon oxidation is as follows [37],

$$2C + O_2 \rightarrow 2CO \text{ --------- } (3\text{-}2)$$

$$2CO + O_2 \rightarrow 2CO_2 \text{ ----- } (3\text{-}3)$$

Since the by-products of these experiments are gases, post treatment was not required. Sample morphology and other properties were characterized in comparison to the sample without etching.

3.4 Material Characterization

CNT mass loading was determined by weighing each Al substrate with the catalyst layer before and after APCVD process, using VWR® Science education RS232 series precision balance. All CNT samples with 2 different carrier gases and samples after KOH and air etching, were examined using Hitachi SU 8230 Scanning Electron Microscope to observe the surface morphology.

There are numerous ways to prepare cell configurations for SC. The capacitance of the electrode samples in this investigation was determined using a custom made three-electrode setup. This system consists of an Ag/AgCl reference electrode with a potential

window of 0 V - 0.8 V, graphite rod as a counter electrode, and sample as the working electrode. 1M aqueous sodium sulfate (Na_2SO_4) solution was employed as the electrolyte of the 3 – electrode system. The used potential window was 0.8 V because of the water electrolysis voltage being 1V. Cyclic voltammetry plots for each sample of two carrier gases and air etched samples were obtained using VSP – 300 electrochemical workstation.

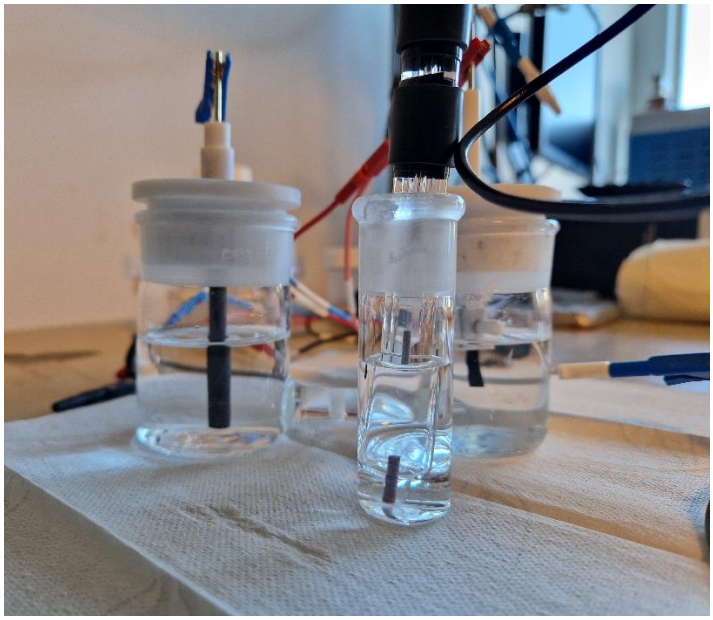

Figure 3-5: 3-electrode cell configuration for the measurement of specific capacitance of the electrodes

Areal capacitance and gravimetric capacitance were calculated by using the equations below.

$$C_{Areal} = \frac{Total\ area\ under\ the\ curve(mA*V)}{2*scan\ rate(\frac{mV}{s})*Area\ of\ the\ electrode(cm2)*potential\ window(V)} \quad \text{----- (3-4)}$$

$$C_{Gravimetric} = \frac{Total\ area\ under\ the\ curve(mA*V)}{2*scan\ rate(\frac{mV}{s})*Active\ mass\ of\ the\ electrode\ (g)*potential\ window(V)} \quad \text{----- (3-5)}$$

At the initial stage of the experiments, because of the availability of excess sputtered samples, one experiment was characterized by coin cell supercapacitor configuration as well. For coin cell configuration, an organic electrolyte with Acetonitrile (AN) 70-80% and N,N-Dimethylpyrrolidinium Tetrafluoroborate（DMP）20-30% (purchased from Jiagnsu

Guotai super power new materials Co. Ltd) and MN GF-5 (purchased from Macherey-Nagel) glass fiber separator was used. Synthesized CNT samples using N_2 as carrier gas were cut in to 1.1cm diameter disks using a die punch and two of these electrodes with a separator in between were used as the electrodes inside coin cell parts. 80µL of the electrolyte was used to soak the electrodes and the separator using a micropipette. Coin cell assembly was done inside the glove box (MBraun – EasyLab) with controlled pressure, O_2 and H_2O vapor environment. After assembling the cell configuration, the whole cell was sealed with 0.9Torr pressure using an MSK-160E crimping/ de-crimping machine for coin cells. The prepared cell is then characterized using VSP – 300 electrochemical workstation to obtain cyclic voltammetry curves.

In addition to calculating the specific capacitance by cyclic voltammetry, coin cell sample was characterized by galvanostatic charge-discharge (GCD) curve as well. The current (I) used for this experiment was 2mA. Capacitance calculation equations for GCD are mentioned in equation 3-6 and 3-7.

$$C_{Gravimetric} = \frac{I\,(mA) \times \Delta t(s)}{m(g) \times \Delta V(V)} \quad \text{----- (3-6)}$$

$$C_{Areal} = \frac{I\,(mA) \times \Delta t(s)}{A(cm2) \times \Delta V(V)} \quad \text{---------- (3-7)}$$

Δt is the time difference in the x axis of the GCD curve and ΔV is the maximum and minimum potential difference which can be obtained by the y axis of the GCD curve. Active mass of the CNT is represented by m and electrode area is represented by A [26].

4 Results and Discussion

4.1 Cost-effective and feasible carrier gas for CNT growth

The synthesis of CNTs using thermal APCVD process requires an intert gas as a carrier gas for two primary reasons. First, carrier gas used to transport the hydrocarbon particles in to the furnace and secondly, it acts as a filler gas to maintain the pressure equivalent to atmospheric pressure inside the tube furnace. Researchers have commonly used Ar and N_2 gases as carrier gas yielding promising results with higher capacitances.

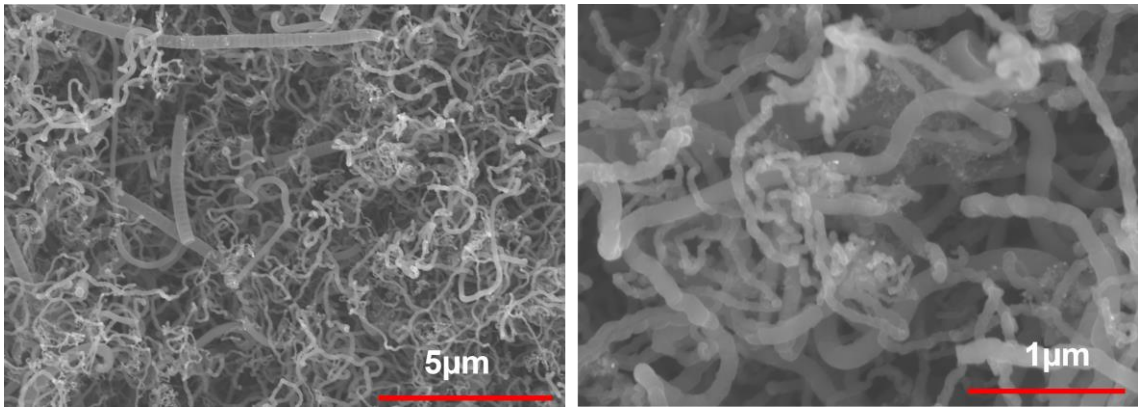

Figure 4-1: Morphology of CNTs synthesized using Ar as the carrier gas with the gas ratio of Ar: H_2: C_2H_2 = 100: 80: 20sccm

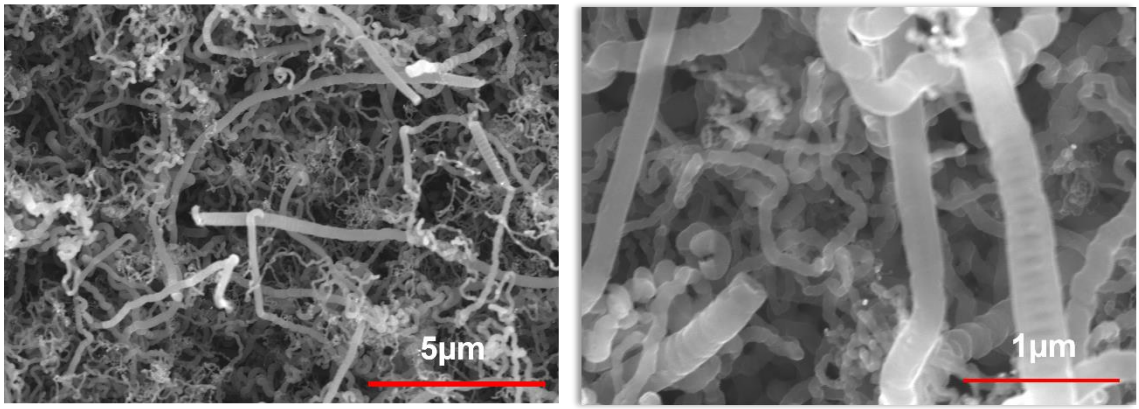

Figure 4-2: Morphology of CNTs synthesized using N_2 as the carrier gas with the gas ratio of N_2: H_2: C_2H_2 = 100: 80: 20sccm

SEM images of the samples synthesized using Ar and N_2 as carrier gases during synthesis of CNTs, as depicted in Figure 4-1 and Figure 4-2, respectively, reveal that the observed

CNT morphology shows similar characteristics, such as the CNT structure and the average diameter of CNTs.

Table 1: Weight of the synthesized CNTs, Areal capacitance and Gravimetric capacitance comparison between CNT synthesized using N_2 and Ar as carrier gases.

	CVD with Ar as carrier gas Ar:H_2:C_2H_2 = 100:80:20	CVD with N_2 as carrier gas N_2:H_2:C_2H_2 = 100:80:20
Mass loading of CNTs mg/cm^2	8	3.23
Specific C_A (µF/cm^2)	35.18	24.66
Specific C_g (F/g)	4.4	7.04

When observing Table 1, the samples synthesized using Ar and N_2 as carrier gas shows approximately similar areal capacitances. However, N_2 gas sample has lower CNT weight hence the gravimetric capacitance is higher compared to Ar sample.

These samples were characterized through FTIR to observe any structural difference or other bonding characteristics. Figure 4-3 FTIR spectra against transmittance has two prominent valleys at 914 cm^{-1} and 2098 cm^{-1} and these two values represent CNT backbone which is in 500 cm^{-1} – 1000 cm^{-1} range and $C \equiv C$ which is in 2000 cm^{-1} – 2400 cm^{-1} range [38]. This confirms that replacing N_2 with Ar will not create any additional functional groups on CNTs and reveal the same characteristics.

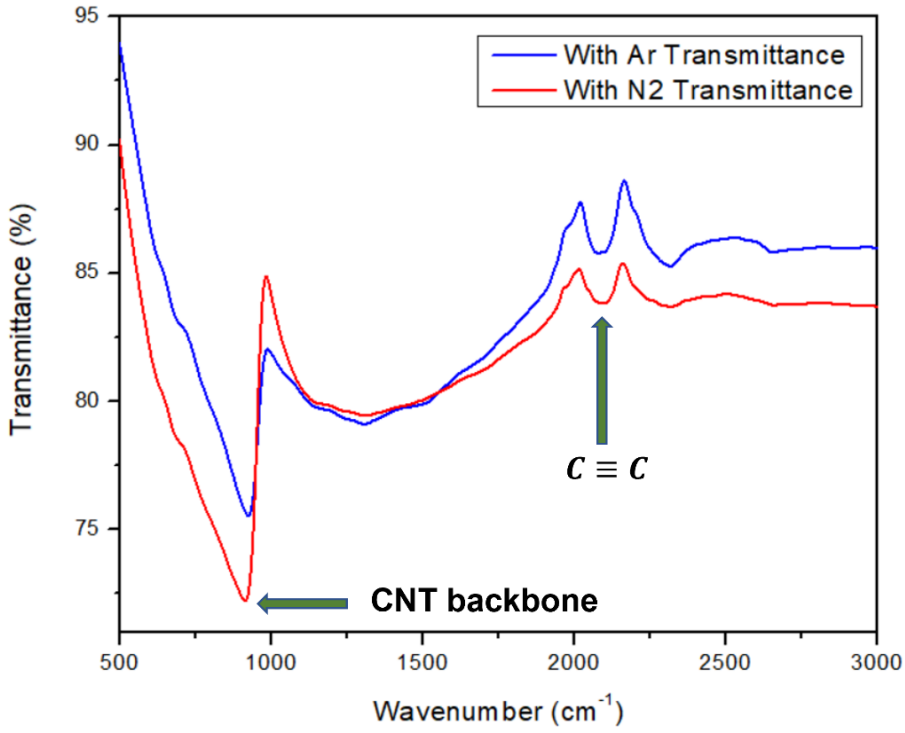

Figure 4-3: FTIR spectra of the samples synthesized with Ar and N_2 as carrier gas.

Therefore, it can be said that using either Ar or N_2 as a carrier gas has the same effect on CNT growth, and since the N_2 is more cost-effective and practical in larger scale production, N_2 is the good option for a carrier gas. Another thing observed was the mass loading of these samples. N_2 samples had a lower mass loading compared to Ar based samples which could be beneficial in applications such as electric car energy storage as having thinner SCs is much easier, and it consumes less space.

4.2 Morphology analysis of KOH etched CNT

To enhance the surface morphology of CNTs to achieve higher capacitance in SC, two methods of etching was followed in this study. Both methods were ex-situ etching methods and one method involved removing the CNTs from the Al substrate after synthesis, while the other was performed with the CNTs still on the Al substrate.

The morphology of ex-situ KOH etched samples was observed using SEM as depicted in Figure 4-4. Appendix contains more SEM morphology images. Upon exposure to high temperature, KOH reacts with C atoms on CNT structure, forming K_2CO_3 and this process makes the CNT structure porous.

In comparison with the pristine CNTs in Figure 4-1 and Figure 4-2, the SEM morphology in Figure 4-4 reveals porous CNTs with the porous areas of the CNT surface is indicated by arrows. These porous regions appear to be indicative of CNT that have been broken along the tubular structure, however, the depth of the porosity was entirely unclear. Additionally, the presence of porous regions possibly depends on the amount of KOH used, as the porosity was observed only in certain CNTs [39].

Even though KOH etching showed a certain degree of porous morphology on CNTs, from the first experiments it was observed that the amount of CNT should be much higher to have successfully etched CNTs after the etching process. The lower CNT mass was completely reacted, and there were no leftover samples after the experiment. CNT powder was light weight therefore, etching under an inert gas flow in a vacuum tube needed to be controlled carefully to have left over product after etching.

Furthermore, this experiment should be done in an inert atmosphere and the whole furnace should be filled with inert gas after removing all the air inside due to carbon reaction with air at high temperatures above 500^{o}C [13]. However, CNTs, even without etching, have entrapped air inside hence, even after filling the furnace with inert gas, this entrapped air may not be completely removed. This entrapped air might react with C atoms at high temperature resulting in no left over etched CNTs.

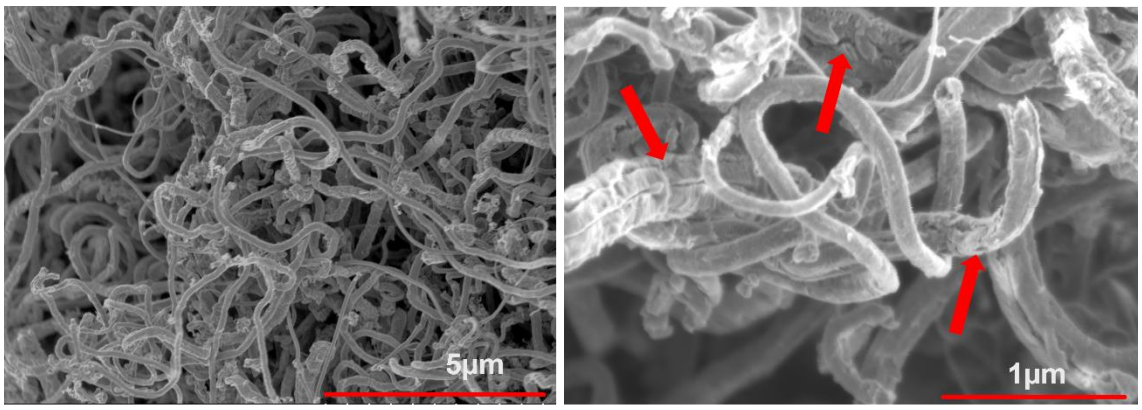

Figure 4-4: CNT morphology after KOH ex-situ etching for using KOH: CNT = 2:1 ratio for duration of 15minutes at 700^{o}C temperature.

KOH is a very reactive chemical at higher temperatures hence the furnace sample boat should be chosen carefully as well. In this study a quartz boat was used to etch which

later found out that quartz boat gets etched by KOH. Additionally, the reaction temperature should be higher than 700°C for the etching reaction to implement, hence the CNTs should be separated from the Al substrate as it is higher than the Al melting temperature.

4.3 Surface area and capacitance improvement by air etching

CNTs synthesized using N_2 as carrier gas on Al subsrate was used for air etching. In comparison with pristin CNTs in Figure 4-1 and Figure 4-2, the morphology observed through SEM of air etched samples has more visible porosity on CNT surface. However, the visible porosity can be observed in 20min and 25min etched samples rather than 10min etched sample. Compared with the morphology of the KOH etched sample in Figure 4-4, the average number of porous regions are higher and porosity is distributed along the tubular structure. This distribution will be an advantage in obtaining a higher specific capacitance in SC.

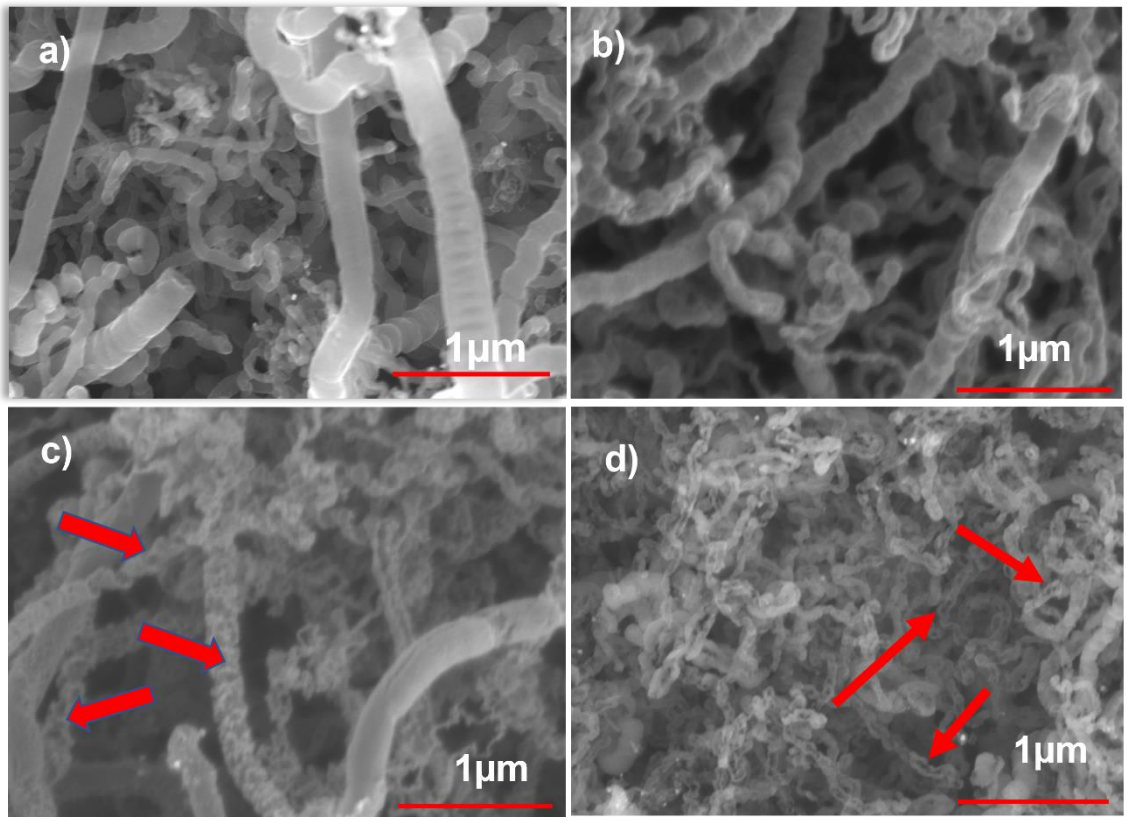

Figure 4-5: Morphology of porous CNTs after air etching at a temperature of 500°C for a) without air etching b)10min c)20min d)25min

Air etching occurs at elevated temperatures by C atoms in the sp^2 hybridized structure of CNTs reacting with O_2 in air as described by equation 3-2 and 3-3. Previous studies have reported that this reaction occurs within the temperature range of 490°C – 650°C, and at the temperatures exceeding this range resulting in complete combustion of CNTs with O_2 which is causing severe damage to the CNT structure [13],[36]. Therefore, in the present study, 500°C was selected as it has been found to result in a significantly good level of porosity at this temperature, while also being within the melting temperature range of Al.

Furthermore, this study investigated the effect of air etching porosity for the specific capacitance in comparison with the pristin CNTs.

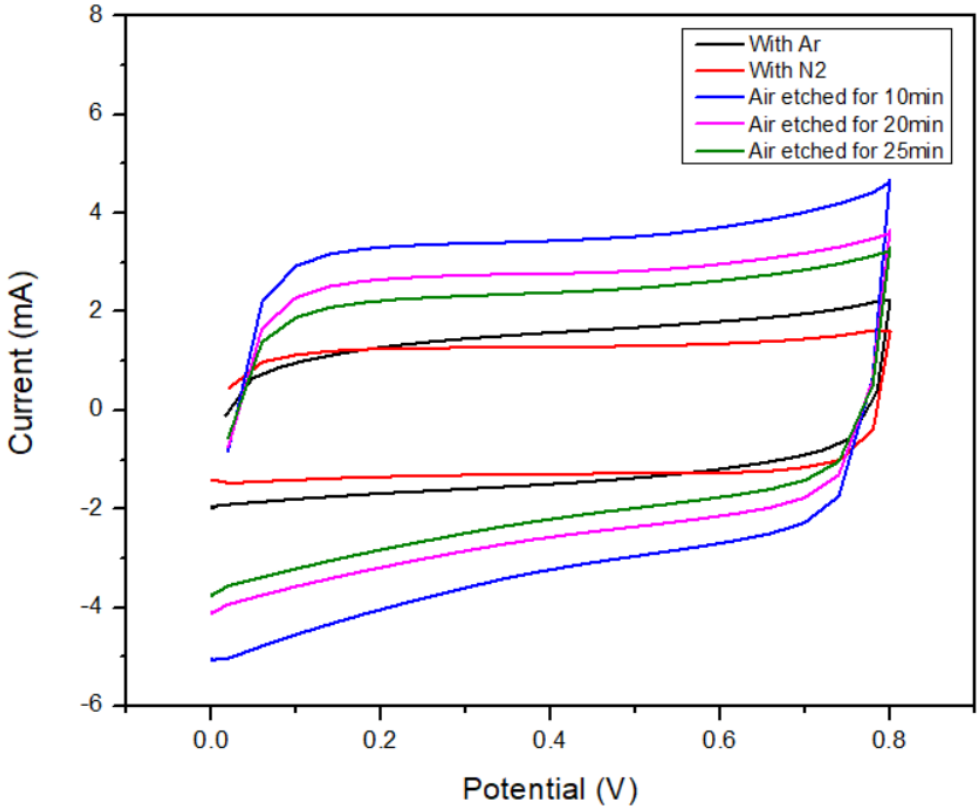

Figure 4-6: CV curves obtained from 3 – Electrode test for air etched samples at different time durations in comparison with pristine CNT synthesized with Ar and N_2 carrier gases at a scan rate of 100mV/s

A prominent characteristic of an ideal supercapacitor is a symmetric rectangular shape in cyclic voltammetry curve, with no evident redox peaks, which indicate the absence of Faraday's redox reactions during the charging and discharging process of the capacitor.

In this scenario, the only driving force for the movement of ions is the electrostatic force that exists between ions and charges in the current collector [40].

Therefore, in a practical supercapacitor, the CV curve is a symmetric semi-rectangular shape as shown in Figure 4-6, which occurs due to the formation of electrical double layer at electrode – electrolyte interface in addition to the electrostatic force [41].

Table 2: Weight of the synthesized CNTs, Areal capacitance and Gravimetric capacitance comparison between pristine CNT synthesized using N_2 as carrier gas and after ex-situ air etching.

	CVD with N_2 as carrier gas N_2:H_2:C_2H_2 = 100:80:20	After CVD air etching at 600°C		
		10min	20min	25min
Mass loading of CNTs mg/cm^2	3.23	1.45	1.29	0.97
Specific C_A µF/cm^2	24.66	70.99	63.31	73.12
Specific C_g F/g	7.04	22.03	19.6	22.6

When observing the capacitance values in Table 2, in comaprison to specific capacitance of pristine CNTs, the specific capacitance of ex-situ air etched samples have increased. Capacitance mainly depends on the accessible surface area of the electrolyte ions. Therefore, when the porosity occurred after air etching on CNT surface, it enables the electrolytic ions to connect with more electrode surface area creating a collection of double layers which can store more charge, thereby increasing the both areal and gravimetric specific capacitances.

Capacitance value dependance over etched time is ploted in Figure 4-7. It can be observed that the capacitance increase with etched time although after a one point it will reduce. This can be explained by over oxidation of C causing severe damage to CNTs hence, the effective surface area reduces [13]. Therefore it can be predicated that if the

duration of etched time increases more than 25 minutes, there's a higher possiblity of reduction of capacitance.

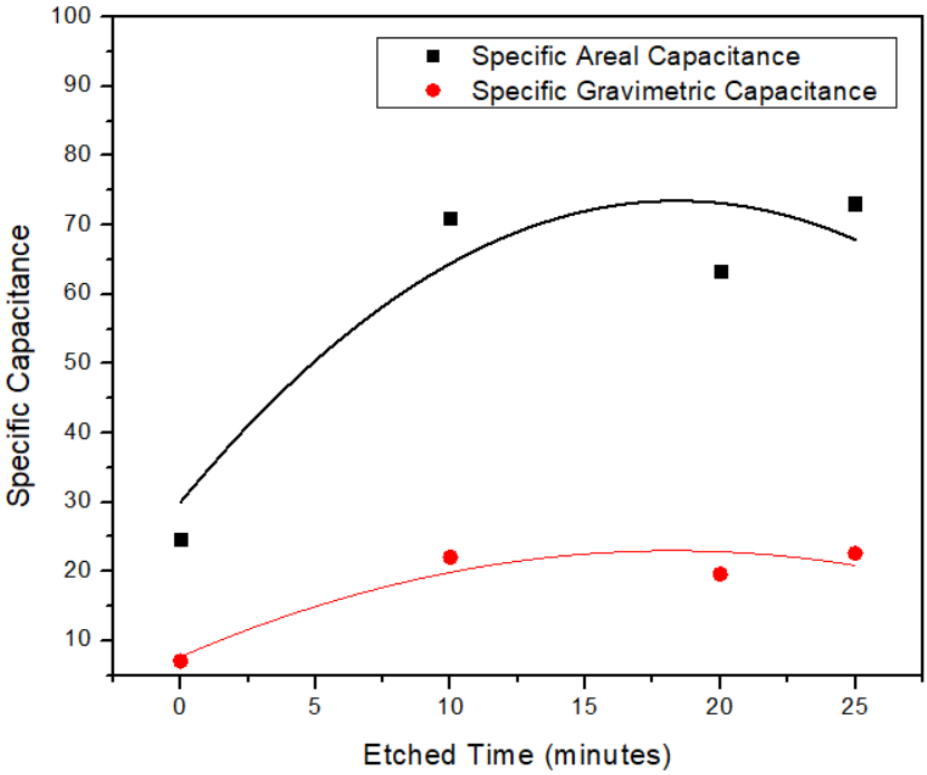

Figure 4-7: Specific areal capacitance(mF/cm^2) and specific gravimetric capacitance (F/g) differences of air etched samples in different durations in comparison with pristine CNTs synthesized by N_2 carrier gas.

Another aspect to consider is the mass loading of CNTs synthesized using N_2 as carrier gas on Al substrate with sputtered Ni as a catalyst layer, is low hence, if the time duration of air etching is long, the possibility of complete combustion will be higher.

In addition to the etching of CNT, air oxidation of CNTs can be used for purification of CNTs [42]. When air reacting with C, the rate of reactivity is higher in amorphous carbon, and structures with pentagons and heptagons, than hexagonal structures which is the stucture of CNT cylindrical wall [36]. Therefore, air etching, in cotrolled manner can first, remove other forms of carbon except CNTs and then react with CNTs resulting porous surface.

4.4 Higher gravimetric capacitance using N_2 as carrier gas

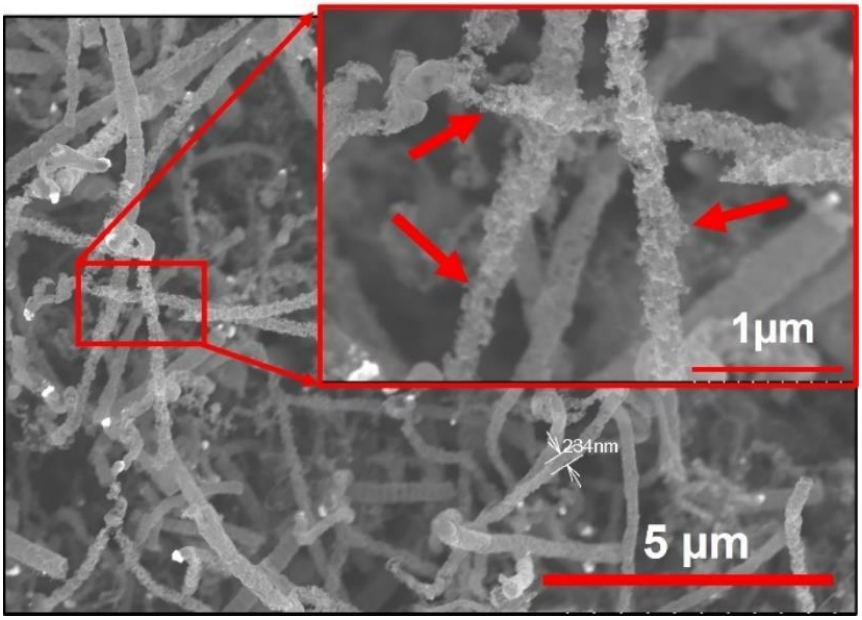

Figure 4-8: CNT deposited on Al substrate with a thickness of 100nm Ni catalyst layer (machine specified planar surface thickness) with a gas ratio of N_2:H_2:C_2H_2 = 100:80:20sccm

Figure 4-8 shows the morphology observed through SEM for CNTs synthesized on Al substrate using the gas composition of N_2:H_2:C_2H_2 = 100:80:20sccm. CNT surface shows a scattered morphology indicating an in-situ etching process has occurred during the synthesis. However, in theory, the only in-situ etching that could happen in this process is N_2 doping, but due to the high bond energy of the triple bond of N_2, it is highly unlikely to produce this scattered surface from thermal APCVD. Refer to Appendix for more SEM morphology done with N_2 as a carrier gas resulted no visible porosity. Also, N_2 doping porosity is mostly in micropore range, therefore, this high porosity is not possible to occur from N_2 doping. Additionally, FTIR spectra for CNT synthesized using N_2 as a carrier gas didn't show any C-N bond peak. Except for scattered morphology of CNTs, thickness of the CNT layer was extremely thin with only 1.03mg/cm^2 mass loading.

An additional factor contributing to the observed morphology could be a probable leakage in the system that allowed O_2-containing air to enter the furnace. The surface morphology effect on CNTs occurred by air etching as observed in Figure 4-5 can be compared with the sample morphology observed in Figure 4-8, which demonstrate

similar structure but to a lesser extent. Repetition of this experiment needed to be investigated furthermore to figure out the reason for these defects.

This sample was characterized with CV measurements to calculate the specific areal and gravimetric capacitances.

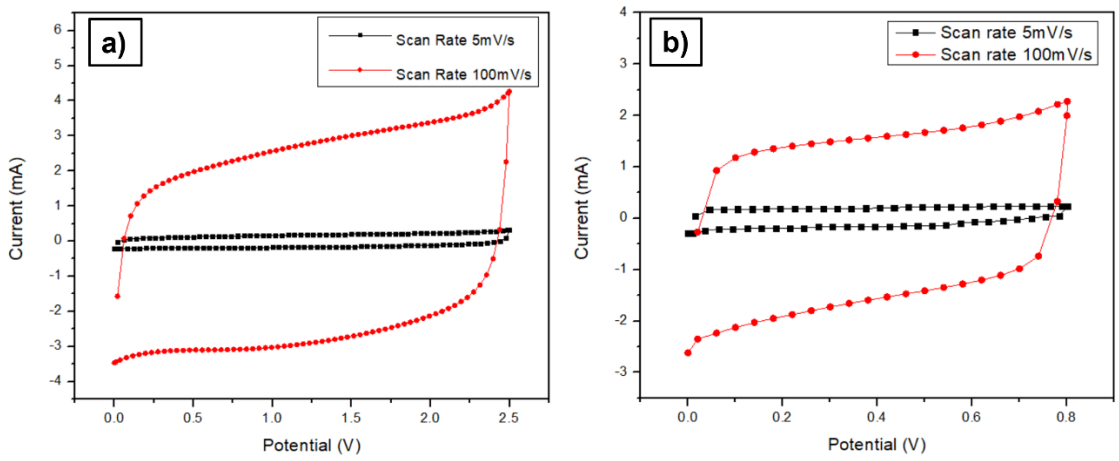

Figure 4-9: a) Coin cell CV curve of the sample in Figure 4-8 for scan rate 5mV/s and 100mV/s using organic electrolyte b) 3 - Electrode CV curve of sample in Figure 4-8 for scan rates 5mV/s and 100mV/s using Na_2SO_4 aqueous electrolyte

Both CV curves from organic electrolyte and Na_2SO_4 electrolyte showed a symmetrical semi-rectangular curve indicating that it contained appropriate practical supercapacitor characteristics.

The selection of appropriate electrolyte is an important factor in the performance of SC. Even though the 3 – electrode test is a convenient method for capacitance measurements as it requires a smaller sample, one of the drawbacks is the relatively high volume of electrolyte required per one cell, that can negatively impact on long-term use and cost. As a result, aqueous electrolytes are commonly employed in 3 – electrode tests due to their cost effectiveness and durability. However, the potential window of an aqueous electrolyte is limited to a value below 1V due to occurrence of water electrolysis at potential windows higher than 1 V. Therefore, in the present experiment, Na_2SO_4 was used as aqueous electrolyte, and 0.8 V was used as the potential window [43].

Due to the availability of larger number of sputtered samples in the initial stage of this study, the sample mentioned in Figure 4-8 was fabricated into a coin cell SC using organic electrolyte. For this organic electrolyte, 2.5 V was chosen as the potential window as the supplier mentioned potential window limitation was 3 V.

The slight variation in the capacitance values between two types of cell configurations can be attributed to this electrolyte potential window limitation. However, it should be noted that, at lower scan rates, the specific capacitance values in both cell configurations were found to be comparable.

Table 3: Specific capacitance and ESR values for 2 different scan rates for Figure 4-8 sample

	Coin cell		3 – electrode test	
Scan rate (mV/s)	5	100	5	100
Specific C_{Areal} (mF/cm^2)	68.37	54.15	68.53	49.49
Specific $C_{Gravimetric}$ (F/g)	66.27	52.47	67.13	48.01
ESR value (Ω)	8.21Ω		4.23Ω	

It can be observed that the use of larger scan rates may pose a challenge to systems with electrolytes with the low ion diffusivity, and electrodes with porous structure, or both as reported in previous studies [44]. The capacitance values for samples were recorded at two different scan rates in two different types of cell configurations are mentioned in Table 3. As expected, the results indicated that the specific capacitance values are higher in 5mV-s scan rate compared to 100mV-s scan rate. At higher scan rates, the diffusion of ions into the porous surface of an electrode is limited, resulting in a reduction of the number of ions available to contribute to the specific capacitance. Therefore, it is advantageous to use lower scan rates to achieve the maximum utilization of electrolytic ions in the generation of capacitance [44].

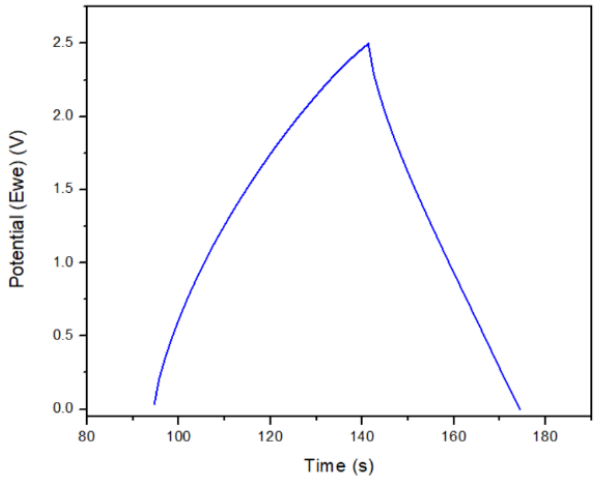

Figure 4-10: Galvanostatic Charge - Discharge curve for sample in Figure 4-8 at 2mA current using organic electrolyte.

It is noteworthy that existing pristine CNT gravimetric capacitances are in range of 10 – 80F/g, depending on the catalyst used [45]. Therefore, the current sample under investigation achieved a gravimetric capacitance of 68 F/g in both cell configurations by cyclic voltammetry, and using GCD under 2mA current calculated specific capacitance using equation 3-6 and 3-7 [26], resulted a 65 F/g gravimetric capacitance, which falls within the high end of the currently existing range.

The energy density and the power density for this supercapacitor can be calculated using the following equations.

$$Energy\ density\ (E_g) = \frac{1}{2} \times C_{Gravimteric} \times (\Delta V)^2 \quad \text{----------4-1}$$

$$Power\ Density\ (P_g) = \frac{E_g}{\Delta t} \times 3600 \quad \text{-------4-2}$$

For the sample in Figure 4-8, the calculated values for energy density are 56.42 $Whkg^{-1}$ and 2.5 kWkg-1 for power density. In existing literature, around 63 $Whkg^{-1}$ was achieved for composite SC with graphene and CNT and hybrid capacitors [46]. Therefore, the energy density acquired for this study can be considered as a promising value. However, future experiments needed to be done for higher energy density and power density values for practical applications.

It is mentioned that the energy density, and power density calculations are more accurate at package level of the supercapacitor cell as these parameters depends on specific parameters of the packaging such as mass of the dead components and cell configuration [47]. Therefore, this value was only calculated for coin cell configuration.

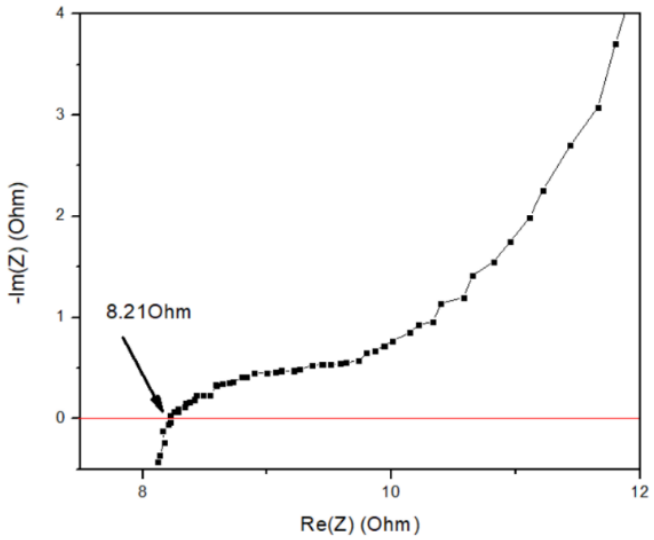

Figure 4-11: Nyquist plot for the sample in Figure 4-8

Nyquist plot can be used to show the internal resistance of a supercapacitor cell. The value where the plot intersect the x-axis represent the real value of the impedance which is considered as the equivalent series resistance (ESR) for a SC cell [47]. For this sample, observed ESR value was 8.21Ω as shown in Figure 4-11 for the coin cell configuration. It was observed that the value of ESR for 3 electrode was 4.23Ω as mentioned in Table 3 which is almost half as the coin cell. Coin cell configuration has 2 electrodes while only one electrode was used in 3 – electrode configuration. This explains the ESR value difference between the 2 methods.

5 Conclusion and Future work

Both Ar and N_2 are shown to be effective carrier gas in the CVD process for synthesizing CNTs since both methods provide similar characteristics in terms of morphology and capacitance. Therefore, replacing Ar with N_2 as a carrier gas will be practical and cost-effective for industrial-scale CNT production. However, it should be noted that CNTs synthesized using N_2 as carrier gas have a lower mass loading, resulting in a comparatively high gravimetric capacitance which may provide an advantage for certain applications such as electric car energy storages. Further investigations need to be done regarding the reason for higher gravimetric capacitance.

In summary, this study suggests that ex-situ etching can enhance the specific capacitance of a supercapacitor by improving the morphology of CNTs. The KOH etching method produces promising porous morphology; however, the high utilizing temperature makes it unsuitable for CNTs synthesized on the Al substrate. On the other hand, air etching at 500^{o}C in a time duration of less than 25 minutes is a promising alternative with high porosity and increased specific capacitance at a temperature less than the substrate melting temperature. Therefore, for CNTs synthesized on an Al substrate, air etching is suitable ex-situ etching method. These findings provided valuable insight into the development of high-performance CNT-based supercapacitors.

Further investigations are required to fully understand the sample synthesized with N_2 as carrier gas which has a high porous morphology and a high gravimetric capacitance. Repetition of the process should be carefully investigated to ensure the reproducibility of the result. Moreover, future studies could explore the combination of air etching during the CNT synthesis sample cooling process, such as introducing a certain amount of O_2 gas into the system along with the N_2 flow. However, it is important to carefully consider the temperature range and O_2 gas flow rate as residual H_2 and C_2H_2 may react with O_2 in the system, and excessive O_2 could potentially damage the synthesized CNTs.

References

[1] Y.-M. Dai, “Surface activation on multi-wall carbon nanotube for electrochemical capacitor applications,” *Appl. Surf. Sci.*, 2012.

[2] R. S. Hastak, P. Sivaraman, D. D. Potphode, K. Shashidhara, and A. B. Samui, “High temperature all solid state supercapacitor based on multi-walled carbon nanotubes and poly[2,5 benzimidazole],” *J. Solid State Electrochem.*, vol. 16, no. 10, pp. 3215–3226, Oct. 2012, doi: 10.1007/s10008-012-1679-6.

[3] Department of Electrical and Electronics Engineering, SRM University, Kattankulathur, India 603203. and Z. S. Iro, “A Brief Review on Electrode Materials for Supercapacitor,” *Int. J. Electrochem. Sci.*, pp. 10628–10643, Dec. 2016, doi: 10.20964/2016.12.50.

[4] Ch. Emmenegger *et al.*, “Investigation of electrochemical double-layer (ECDL) capacitors electrodes based on carbon nanotubes and activated carbon materials,” *J. Power Sources*, vol. 124, no. 1, pp. 321–329, Oct. 2003, doi: 10.1016/S0378-7753(03)00590-1.

[5] Q. Jiang, M.-Z. Qu, B.-L. Zhang, and Z.-L. Yu, “Preparation of activated carbon nanotubes,” *Carbon*, vol. 40, no. 14, pp. 2743–2745, 2002, doi: 10.1016/S0008-6223(02)00208-7.

[6] X. Li and B. Wei, “Supercapacitors based on nanostructured carbon,” *Nano Energy*, vol. 2, no. 2, pp. 159–173, Mar. 2013, doi: 10.1016/j.nanoen.2012.09.008.

[7] P. Ayala, R. Arenal, M. Rümmeli, A. Rubio, and T. Pichler, “The doping of carbon nanotubes with nitrogen and their potential applications,” *Carbon*, vol. 48, no. 3, pp. 575–586, Mar. 2010, doi: 10.1016/j.carbon.2009.10.009.

[8] Y. G. Lin, Y. K. Hsu, C. T. Wu, S. Y. Chen, K. H. Chen, and L. C. Chen, “Effects of nitrogen-doping on the microstructure, bonding and electrochemical activity of carbon nanotubes,” *Diam. Relat. Mater.*, vol. 18, no. 2–3, pp. 433–437, Feb. 2009, doi: 10.1016/j.diamond.2008.09.009.

[9] X. Zhang, Y. Hao, and W. Zhong, “Boron-doped helical carbon nanotubes: lightweight and efficient microwave absorbers,” *J. Mater. Sci. Mater. Electron.*, vol. 32, no. 21, pp. 26161–26172, Nov. 2021, doi: 10.1007/s10854-021-06560-8.

[10] R. Czerw *et al.*, “Identification of Electron Donor States in N-Doped Carbon Nanotubes,” *Nano Lett.*, vol. 1, no. 9, pp. 457–460, Sep. 2001, doi: 10.1021/nl015549q.

[11] E. Raymundo-Piñero, P. Azaïs, T. Cacciaguerra, D. Cazorla-Amorós, A. Linares-Solano, and F. Béguin, “KOH and NaOH activation mechanisms of multiwalled carbon nanotubes with different structural organisation,” *Carbon*, vol. 43, no. 4, pp. 786–795, Jan. 2005, doi: 10.1016/j.carbon.2004.11.005.

[12] X. Zhang, “Mechanisms of pore formation on multi-wall carbon nanotubes by KOH activation,” *Microporous Mesoporous Mater.*, 2015.

[13] C. Li *et al.*, “Oxidation of multiwalled carbon nanotubes by air: benefits for electric double layer capacitors,” *Powder Technol.*, vol. 142, no. 2–3, pp. 175–179, Apr. 2004, doi: 10.1016/j.powtec.2004.04.037.

[14] W. Zhao *et al.*, “Controlled Air-Etching Synthesis of Porous-Carbon Nanotube Aerogels with Ultrafast Charging at 1000 A g−1,” 2018.

[15] R. Kavian, A. Vicenzo, and M. Bestetti, “Growth of carbon nanotubes on aluminium foil for supercapacitors electrodes,” *J. Mater. Sci.*, vol. 46, no. 5, pp. 1487–1493, Mar. 2011, doi: 10.1007/s10853-010-4950-1.

[16] C. J. Lee, J. Park, and J. A. Yu, “Catalyst effect on carbon nanotubes synthesized by thermal chemical vapor deposition,” *Chem. Phys. Lett.*, vol. 360, no. 3–4, pp. 250–255, Jul. 2002, doi: 10.1016/S0009-2614(02)00831-X.
[17] E. S. Kudinova, E. A. Vorobyeva, N. A. Ivanova, V. V. Tishkin, and O. K. Alekseeva, “A Magnetron Sputtering Method for the Application of the Ni Catalyst for the Synthesis Process of Carbon Nanotube Arrays,” *Nanotechnologies Russ.*, vol. 15, no. 11–12, pp. 715–722, Nov. 2020, doi: 10.1134/S1995078020060129.
[18] M. S. Dresselhaus, G. Dresselhaus, P. C. Eklund, and A. M. Rao, *The Physics of Fullerene-Based and Fullerene-Related Materials*. Springer, Dordrecht, 2000.
[19] S. I. Cha, K. T. Kim, K. H. Lee, C. B. Mo, Y. J. Jeong, and S. H. Hong, “Mechanical and electrical properties of cross-linked carbon nanotubes,” *Carbon*, vol. 46, no. 3, pp. 482–488, Mar. 2008, doi: 10.1016/j.carbon.2007.12.023.
[20] R. Baker, “Nucleation and growth of carbon deposits from the nickel catalyzed decomposition of acetylene,” *J. Catal.*, vol. 26, no. 1, pp. 51–62, Jul. 1972, doi: 10.1016/0021-9517(72)90032-2.
[21] G. P. Gakis, S. Termine, A.-F. A. Trompeta, I. G. Aviziotis, and C. A. Charitidis, “Unraveling the mechanisms of carbon nanotube growth by chemical vapor deposition,” *Chem. Eng. J.*, vol. 445, p. 136807, Oct. 2022, doi: 10.1016/j.cej.2022.136807.
[22] M. Winter and R. J. Brodd, “What Are Batteries, Fuel Cells, and Supercapacitors?,” *Chem. Rev.*, vol. 104, no. 10, pp. 4245–4270, Oct. 2004, doi: 10.1021/cr020730k.
[23] W. Raza *et al.*, “Recent advancements in supercapacitor technology,” *Nano Energy*, vol. 52, pp. 441–473, Oct. 2018, doi: 10.1016/j.nanoen.2018.08.013.
[24] M. Lu, F. Beguin, and E. Frackowiak, “Supercapacitors: Materials, Systems and Applications,” in *Supercapacitors*, 1st ed.in Materials for Sustainable Energy and Development Ser. John Wiley & Sons, Incorporated, 2013, pp. 39–48.
[25] R. Burt, G. Birkett, and X. S. Zhao, “A review of molecular modelling of electric double layer capacitors,” *Phys. Chem. Chem. Phys.*, vol. 16, no. 14, p. 6519, 2014, doi: 10.1039/c3cp55186e.
[26] H. Li, J. Wang, Q. Chu, Z. Wang, F. Zhang, and S. Wang, “Theoretical and experimental specific capacitance of polyaniline in sulfuric acid,” *J. Power Sources*, vol. 190, no. 2, pp. 578–586, May 2009, doi: 10.1016/j.jpowsour.2009.01.052.
[27] K. Wang, “Dry Etching - MFA4000-1 22V Microfabrication Technology,” University of South-Eastern Norway.
[28] F. O. Jones and K. O. Wood, “The melting point of thin aluminium films,” *Br. J. Appl. Phys.*, vol. 15, no. 2, pp. 185–187, Feb. 1964, doi: 10.1088/0508-3443/15/2/310.
[29] T. P. Mofokeng, Z. N. Tetana, and K. I. Ozoemena, “Defective 3D nitrogen-doped carbon nanotube-carbon fibre networks for high-performance supercapacitor: Transformative role of nitrogen-doping from surface-confined to diffusive kinetics,” *Carbon*, vol. 169, pp. 312–326, Nov. 2020, doi: 10.1016/j.carbon.2020.07.049.
[30] M. Zięzio, B. Charmas, K. Jedynak, M. Hawryluk, and K. Kucio, “Preparation and characterization of activated carbons obtained from the waste materials impregnated with phosphoric acid(V),” *Appl. Nanosci.*, vol. 10, no. 12, pp. 4703–4716, Dec. 2020, doi: 10.1007/s13204-020-01419-6.
[31] M.-K. Seo and S.-J. Park, “Influence of air-oxidation on electric double layer capacitances of multi-walled carbon nanotube electrodes,” *Curr. Appl. Phys.*, vol. 10, no. 1, pp. 241–244, Jan. 2010, doi: 10.1016/j.cap.2009.05.031.

[32] Z. Wang, Q. Zhao, L. Tong, and J. Zhang, “Investigation of Etching Behavior of Single-Walled Carbon Nanotubes Using Different Etchants,” *J. Phys. Chem. C*, vol. 121, no. 49, pp. 27655–27663, Dec. 2017, doi: 10.1021/acs.jpcc.7b06653.
[33] A. Li-Pook-Than, J. Lefebvre, and P. Finnie, “Type- and Species-Selective Air Etching of Single-Walled Carbon Nanotubes Tracked with *in Situ* Raman Spectroscopy,” *ACS Nano*, vol. 7, no. 8, pp. 6507–6521, Aug. 2013, doi: 10.1021/nn402412t.
[34] Y. A. Iijima, “Preparation of Carbon Nanotubes by Arc-Discharge Evaporation,” *Jpn. J. Appl. Phys.*, vol. 32, no. 1A, p. L107, Jan. 1993, doi: 10.1143/JJAP.32.L107.
[35] D. T. Colbert *et al.*, “Growth and Sintering of Fullerene Nanotubes,” *Science*, vol. 266, no. 5188, pp. 1218–1222, Nov. 1994, doi: 10.1126/science.266.5188.1218.
[36] Y. S. Park *et al.*, “High yield purification of multiwalled carbon nanotubes by selective oxidation during thermal annealing,” *Carbon*, vol. 39, no. 5, pp. 655–661, Apr. 2001, doi: 10.1016/S0008-6223(00)00152-4.
[37] S. Ahmed, M. H. Back, and J. M. Roscoe, “A kinetic model for the low temperature oxidation of carbon: I,” *Combust. Flame*, vol. 70, no. 1, pp. 1–16, Oct. 1987, doi: 10.1016/0010-2180(87)90155-6.
[38] V. Ţucureanu, A. Matei, and A. M. Avram, “FTIR Spectroscopy for Carbon Family Study,” *Crit. Rev. Anal. Chem.*, vol. 46, no. 6, pp. 502–520, Nov. 2016, doi: 10.1080/10408347.2016.1157013.
[39] B. Xu *et al.*, “Competitive effect of KOH activation on the electrochemical performances of carbon nanotubes for EDLC: Balance between porosity and conductivity,” *Electrochimica Acta*, vol. 53, no. 26, pp. 7730–7735, Nov. 2008, doi: 10.1016/j.electacta.2008.05.033.
[40] S. Aderyani, P. Flouda, S. A. Shah, M. J. Green, J. L. Lutkenhaus, and H. Ardebili, “Simulation of cyclic voltammetry in structural supercapacitors with pseudocapacitance behavior,” *Electrochimica Acta*, vol. 390, p. 138822, Sep. 2021, doi: 10.1016/j.electacta.2021.138822.
[41] A. J. Bard and L. R. Faulkner, *Electrochemical methods: fundamentals and applications*, 2nd ed. New York: Wiley, 2001.
[42] J.-M. Moon, K. H. An, Y. H. Lee, Y. S. Park, D. J. Bae, and G.-S. Park, “High-Yield Purification Process of Singlewalled Carbon Nanotubes,” *J. Phys. Chem. B*, vol. 105, no. 24, pp. 5677–5681, Jun. 2001, doi: 10.1021/jp0102365.
[43] A. Virya, J. Abella, A. Grindal, and K. Lian, “Na2SO4-Polyacrylamide Electrolytes and Enabled Solid-State Electrochemical Capacitors,” *Batter. Supercaps*, vol. 3, no. 2, pp. 194–200, Oct. 2019, doi: 10.1002/batt.201900127.
[44] D. M. Morales and M. Risch, “Seven Steps to Reliable Cyclic Voltammetry Measurements for the Determination of Double Layer Capacitance,” Chemistry, preprint, Mar. 2021. doi: 10.26434/chemrxiv.13311752.v2.
[45] E. Frackowiak, S. Delpeux, K. Jurewicz, K. Szostak, D. Cazorla-Amoros, and F. Béguin, “Enhanced capacitance of carbon nanotubes through chemical activation,” *Chem. Phys. Lett.*, vol. 361, no. 1–2, pp. 35–41, Jul. 2002, doi: 10.1016/S0009-2614(02)00684-X.
[46] Q. Cheng, J. Tang, J. Ma, H. Zhang, N. Shinya, and L.-C. Qin, “Graphene and carbon nanotube composite electrodes for supercapacitors with ultra-high energy density,” *Phys. Chem. Chem. Phys.*, vol. 13, no. 39, p. 17615, 2011, doi: 10.1039/c1cp21910c.
[47] M. D. Stoller and R. S. Ruoff, “Best practice methods for determining an electrode material’s performance for ultracapacitors,” *Energy Environ. Sci.*, vol. 3, no. 9, p. 1294, 2010, doi: 10.1039/c0ee00074d.

List of Figures

List of Tables

Appendix

The first approach of this study was focused on in-situ etching of CNT by N_2 doping using N_2 gas at 600°C in APCVD. Few experiments were followed for observing the possibility of this assumption which finally concluded that the N_2 bond strength cannot be broken by thermal energy at 600°C. SEM morphology observed of these samples didn't show any porosity on CNT surface.

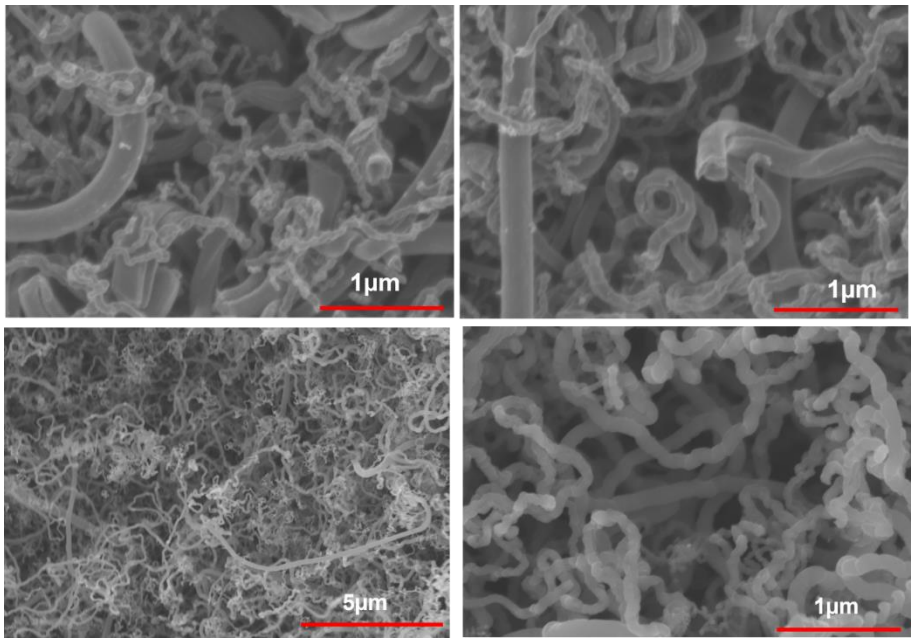

Figure 0-1: CNT synthesized using N_2 as a carrier gas on Al substrate with sputtered Ni catalyst layer.

KOH etched CNT morphology – Additional SEM images